Article citation info:
Kadhim ZH, Hammed L, Rahima FA, Ridha AM. Elastohydrodynamic analysis of a journal bearing with different grade oils considering thermal and cavitation effects using CFD-FSI. Diagnostyka. 2023;24(2):2023213. https://doi.org/10.29354/diag/166102.

DIAGNOSTYKA, 2023, Vol. 24, No. 2

e-ISSN 2449-5220
DOI: 10.29354/diag/166102

ELASTOHYDRODYNAMIC ANALYSIS OF A JOURNAL BEARING WITH DIFFERENT GRADE OILS CONSIDERING THERMAL AND CAVITATION EFFECTS USING CFD-FSI

Zainab H KADHIM [1,*], Lekaa HAMMED [2], Fatima A RAHIMA [3], Ali Mohammed RIDHA [4,5]

[1] Department of Mechanical Power Engineering, Al-Amarah University College, Maysan, Iraq
[2] College of Engineering, Department of Mechanical Engineering, University of Babylon, Babylon, Iraq
[3] Department of Petroleum Engineering, Al-Amarah University College, Maysan, Iraq
[4] Medical Instrumentation Techniques Engineering, Alhussain University College, Karbala, 56001, Iraq
[5] Branch of Physiology and Medical Physics, College of Medicine, University of Al-Ameed, Karbala, 56001, Iraq
[*] Corresponding author, e-mail: zaynab.hafid@alamarahuc.edu.iq

Abstract

This paper investigates a three-dimensional CFD analysis of hydrodynamic journal bearing performance for two different available types of lubricants, SEA 10W50 and SEA 15W40, considering thermal, elastic deformation, and cavitation effects. A 3-dimensional CFD model founded on continuity, momentum, energy, in addition elasticity equations has been implemented. The analysis is performed for a bearing with different journal speeds (1000-3000rpm) and eccentricity ratios (0.1-0.9). The cavitation effect was considered using the model of Zwart–Gerber–Balamri multiphase flow model. The bearing material elastic deformation was considered by implementing the two-way FSI technique through ANSYS-FLUENT 2019 R2. A comparative study of the oil film temperature, thermal pressure, also the load capacity by the bearing has been performed. By comparing the current work's oil film temperature results with those obtained by Ferron et al (1983), with a maximum deviation between the results not exceeding 3 percent, the mathematical model was validated. The findings demonstrate that, once the cavitation consequence is taken into account, the lubricant film pressure decreases. Furthermore, at what time the bearing rotates at greater eccentricity ratios and rotational speeds, more deformation material of the bearing is seen. The current research may help in predicting the bearing performance parameters in real-world situations.

Keywords: journal bearing, hydrodynamic lubrication, thermal effect, elastic deformation, cavitation effect, CFD

List of Symbols/Acronyms

a_{nue} – The volume fraction of the nucleation site which can be taken as 5×10^{-4}
c – Radial clearance [m]
c_p – Thermal conductivity of base oil [$J/kg\ °C$]
D – Journal or Shaft diameter [m]
E – Eccentricity between shaft and bearing [m]
f – Coefficient of friction
F_{evap} – The coefficient of condensation which can be taken as 0.01
F_{cond} – The coefficient of evaporation which can be taken as 50
F_{fr} – Friction force [N]
THD – Thermohydrodynamic
TEDH – Thermoelastohydrodynamic
h – Film thickness [m]
Δh – Relative rigid displacement for the two bearing surfaces
k – Thermal conductivity [W/m*°C]
L – Length of the bearing [m]
L/D – Aspect ratio
N – Speed of rotation [RPM]
Ne, Nc – Mass transfer source terms connected to the growth and collapse of the vapor bubbles respectively
O' – Bearing center
O – Shaft center
p – This pressure in the local fluid film [N/m^2]
p_b – Bubble surface pressure
PV – Pressure of vaporization [Pa]
P_v – Saturation pressure of the fluid [Pa]

1. INTRODUCTION

Journal bearings are frequently used in the transmission of heavy loads at a constant rotational speed. One of the most effective types of journals bearing designs is one with hydrodynamic lubrication. Because of their higher performance, difficult damping, besides comfort of manufacture, various configurations of these bearings were widely used in engineering applications [18]. They can be used to support the turbine/generator unit in hydropower plants, as well as many revolving

machines that have at least one rotating section that must be isolated from the machine's stationary portion. The lubricant is used to keep the two surfaces from rubbing against each other by forming a thin film that can be sheared without harming the surfaces. On experimental bases, Nour Marey (2019) [1] investigated the impacts of performing pressure distribution within the hydrodynamic journal bearing. The experiment work included the use of a variety of lubrication oils, including SEA 20W50, SEA 10W40, and SEA 5W30, in order to determine their unique roles in deciding whether lubrication is hydrodynamic or hydrostatic. The pressure behavior of several lubricants within the hydrodynamic journal bearing at various speeds ranging from 50 to 400 RPM under constant loads had been studied. The maximum film pressure ratio was found to be 0.2, 0.6, and 0.3 for the bearing lubricated with SEA 20W50, SEA 10W40, and SEA 5W30 lubricants respectively at a maximum speed of 400 RPM. The effects of the friction and wear behavior of journal-bearing material were examined by Baskar and Sriram (2014) [2] using a pin on disc wear tester with three changed lubricating oils, namely lubricating oil (SAE20W40), rapeseed oil (CMRO), and chemically modified rapeseed oil with Nano CuO. An extreme load of 200 N too sliding speeds ranging from 2 to 10 m/s were used in wear tests. According to the findings, lubricating oils and sliding conditions had an impact on how much friction and wear the journal bearing material exhibited. The journal bearing material for CMRO with Nano CuO has a lower friction coefficient than the two other oils. When the bearing was lubricated 20W40 and CMRO, it was observed that the journal bearing components wore out more quickly.

According to Lorenz et al. (2017) [3], The geometry of the contacting component surfaces and the characteristics of the lubricating fluid must both be taken into account when forecasting the wear and power loss of journal bearings in internal combustion engines. A common modeling approach for this objective is a Reynolds-averaged equation with laminar flow conditions. It displays a model for the temperature distribution of the lubricant and the bearings. The thermal contact characteristics between these domains are also included. The effect of oil film temperature on oil film viscosity and, consequently, load-carrying capability is demonstrated. The thermohydrodynamic investigation of an elliptic bearing lubricated through various oils was carried out by Chauhan et al. in 2010[4]. Studies have been done on the load supported thru the bearing, thermal pressure, then lubricant temperature rise. It be situated discovered that the minute the bearing is oiled by oil that has the highest viscosity, the load it can support increases. The influence of viscoelastic qualities of multigrade oils on lubrication characteristics was examined by Williamson et al. (1997) [5]. investigated the rheomelectrical properties of different multigrid oils with similar shear viscosity responses. The obtained results show that the viscoelasticity produces measurable and beneficial effects on lubrication characteristics at the higher eccentricity ratios. Rasep et al. [6] (2021) used CFD technique to investigate the effect of cavitation on the journal bearing performance when it was lubricated with engine oil, palm oil, and water. The importance of including the cavitation effect was demonstrated. Muchammad et al. [7](2021) studied the effects of Mechanical also thermal deformations taking place the performance of the plain bearing with iso-viscous boundary conditions based on CFD and FSI techniques. It was demonstrated that the elastic and thermal deformations of the bearing body had an extreme effect on the bearing performance. A fresh method was used by Bekir Sadik Unlu and Enver Atik (2019) [8] to investigate the friction coefficient of bronze radial bearings. According to the results, the lubricated test surroundings have a small friction coefficient and little wear rate, in contrast to the dry test conditions' high friction coefficient and high wear. Liu et al. (2010) [9] proposed CFD-FSI method to perform elasto-hydrodynamic analyses on a rotor-bearing system. It was shown that the CFD-FSI Approach produces more accurate results for rotor-bearing elastohydrodynamic and hydro-dynamic analyses. The results depict that the elastic deformation had a significant impact on the rotor-bearing system. For a thermohydrodynamic analysis of a circular journal bearing, Singla et al. (2014) [10] employed Computational Fluid Dynamics techniques and the ANSYS FLUENT software. The maximum pressure and rising lubricant temperature that occurs when the viscosity is maintained have been shown to have an impact on the bearing's ability to carry loads. The lubrication performance of journal bearings was examined by Chen et al. (2019) [11] using the fluid-structure coupling method, which took into account realistic structures like cavitation in addition distortion. In the numerical analysis, the performance of journal bearings with various groove shapes was examined in relation to eccentricity ratio, rotating speed, and oil-film thinness. As a result, as the bearing operates at higher eccentricity ratio and rotational speed, the peak pressure rises. Although it is negligible in this work for the steel material, the twist of the solid construction at the fluid-structure boundary is significant and cannot be disregarded for elastic materials. The primary objective of the current research is to conduct a CFD analysis for the elastohydrodynamic performance of bearings oiled by several oil grades that be situated currently arranged the market. The temperature of the oil film has been predicted using a three-dimensional energy equation. The bearing's load and thermal oil film pressure have been presented.

2. CFD MODEL

2.1. Bearing dimensions

The current study was carried out using the journal-bearing per the geometry revealed in figure

1. Table 1 shows the bearing geometrical and operational features, as well as the corporeal and thermal possessions of the oil utilized. The bearing eccentricity is thought to be regulated by the pressure generated in the bearing's effective zone until the generated load equalizes the externally applied load.

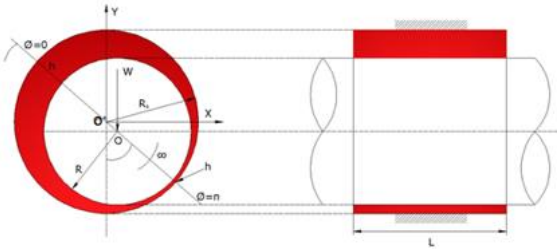

Fig. 1. Hydrodynamic journal bearing geometry

Table 1. Bearings geometrical and operational properties. [12]

Parameters	Units	Values
L/D		0.5
R	mm	50
R_b	mm	50.2
$\boldsymbol{\varepsilon}$		0.1-0.9
$\emptyset$	$Degree$	56
$\boldsymbol{N}$	r/min	1000-3000
c	mm	0.2
μ for SAE 10W50	$N\,s/m^2$	0.0544
μ for SAE 15W40	$N\,s/m^2$	0.0125
$\boldsymbol{P_V}$	Pa	29185
c_p	$J/(kg.K)$	2000
k	$W/(m.K)$	0.12
E	MPa	200000
Bearing length	mm	100

2.2. Governing equations

The following are the mass conservation equations governing the lubricant flow within the journal bearing.

$$\mu = \mu_o \exp\left[-\beta(T - T_{in})\right] \quad (1)$$

2.2.1 Continuity equation [13]

$$\partial u/\partial x + \partial v/\partial y + \partial w/\partial z = 0 \quad (2)$$

2.2.2 Equations of momentum [13]

In this learning, the Navier – Stokes equivalence is used:

$$\frac{\partial}{\partial t}(\rho.\vec{v}) + \nabla(\rho.\vec{v}.\vec{v}) = -\nabla P + \nabla(\bar{\bar{\tau}}) + \rho.+\vec{F} \quad (3)$$

anywhere

P is the pressure of static (N/m^2)

$\bar{\bar{\tau}}$ *is the stress tensor which can be written as*:

$$\bar{\bar{\tau}} = \mu\left[(\nabla.\vec{v} + \nabla.\vec{v}^T) - \frac{2}{3}\nabla \times \vec{v}.I\right] \quad (4)$$

$\vec{F}$ is the force of body.

$\rho.g$ is the force of gravitational.

2.2.2 Equations of energy [13]

By resolving the ensuing steady-state and it is possible to calculate the temperature of the oil layer using the incompressible energy equation:

$$\rho C_p\left(u \cdot \frac{\partial T}{\partial x} + w \cdot \frac{\partial T}{\partial z}\right) = \frac{\partial}{\partial y}\left(K\frac{\partial T}{\partial y}\right) + \mu\left[\left(\frac{\partial u}{\partial y}\right)^2 + \left(\frac{\partial w}{\partial y}\right)^2\right] \quad (5)$$

where

μ is the lubricant viscosity which can be located expressed as a meaning of oil film temperature as follow:

$$\mu = \mu_o \exp\left[-\beta(T - T_{in})\right] \quad (6)$$

μ_o be located the oil viscosity on the temperature of ambient (Pa.s)

T_{in} inlet oil temperature (°C)

2.3. Cavitation model

The influence of oil film cavitation on the bearing performance was considered using the following vapor transport equation [14]:

$$\frac{\partial}{\partial t}(a_v, \rho_v) + \nabla(a_v \cdot \rho_v \cdot v_v) = N_z - N_h \quad (7)$$

N_z also N_h are responsible designed for the mass transference in the cavitated zone among the fluid and vapor stages[18]. Zwart-Gerber cavitation model can be located used to calculate Nz and Nh [13]:

If $p < p_v$

$$N_z = F_{evap} \cdot \frac{3 \cdot a_{nue}(1 - a_v) \cdot \rho_v}{R_{bc}} \cdot \sqrt{\frac{2}{3} \cdot \frac{p_v - p}{\rho_l}} \quad (8)$$

If $p \geqslant p_v$

$$N_h = F_{cond} \frac{3 \cdot a_v \cdot \rho_v}{R_{bc}} \cdot \sqrt{\frac{2}{3} \cdot \frac{p - p_v}{\rho_l}} \quad (9)$$

The generalized Rayleigh-Plesset equation[13] can be used to explain R_{bc}, which is the radius of the bubble.

$$R_{bc}\frac{d^2R_{bc}}{dt^2} + \frac{3}{2}\left(\frac{dR_{bc}}{dt}\right)^2 = \frac{p_b - p}{\rho_l} - \frac{2\sigma}{\rho_l \cdot R_{bc}} - 4 \cdot \frac{\mu_l}{\rho_l \cdot R_{bc}} \cdot \frac{dR_{bc}}{dt} \quad (10)$$

Equation (9) can be rewritten as follows, excluding the second-order and surface tension forces terms:

$$\frac{dR_{bc}}{dt} = \sqrt{\frac{2}{3} \cdot \frac{p_b - p}{\rho_l}} \quad (11)$$

2.4. Fluid-structure interaction model

According to the fluid-solid domain interaction, fluid pressure may impose a force that extends over the fluid-structure boundary, causing the journal bearing to move or deform [17]. The journal bearing's elasto-hydrodynamic lubrication is analyzed using the ANSYS-FLUENT program. The boundary conditions for fluid structure interactions are displacement compatibility, traction equilibrium, and temperature equivalence. They can be stated as:

$$\begin{aligned} d_f &= d_s \\ n \cdot \tau_f &= n \cdot \tau_s \\ T_f &= T_s \end{aligned} \quad (12)$$

where the letters d stand for displacement, T for temperature, and τ for stress, respectively.

2.5. Thickness of the lubricant film model

The fluid-construction interfaces' comparative displacement in the fluid domain is consistent with that in the solid domain. If the elastic deformation of rigid bodies and bearing surfaces is taken into consideration, the distance between the rotor-lubricant interface and the bearing-lubricant interface, as provided by [17], can be described as the film thickness.

$$h = c + \Delta h + \delta \tag{13}$$

where:

c is the space left between the bearing and the journal.

Δh is the two bearing surfaces' comparatively inflexible displacement.

δ The two bearing sides' combined flexible deformation is described by.

3. MESH GENERATION

The journal is depicted as a moving wall with absolute rotational speed, whereas the bearing is modeled as a stationary wall. The fluid domain was meshed using the CFD technique using hexahedral cubicles through a total of 525048 besides an size of element of 0.3 mm, as shown in table 2 and figure 2(a-c). The lubricant film was separated into trio layers in a radial fashion. The eccentricity also angle attitude values are used to agree the start of the shaft axis. By a convergence tolerance of 10-3 and 1000 iterations, the SIMPLEC algorithm was used to solve the governing equations iteratively.

Table 2. The fluid domain analysis results at various mesh grid densities.

Body size	Mesh layers	Aspect ratio	Element number	Pressure	load
0.9	3	66.915	59136	1259810	1941.0731
0.8	3	59.483	74844	1259740	1943.278
0.7	3	52.114	97632	1259990	1945.2413
0.6	3	44.955	132048	1260204	1947.0573
0.5	3	37.273	189600	1260531	1949.0403
0.4	3	29.894	295500	1260449	1950.3141
0.3	3	22.478	525048	1260704	1951.9634
0.2	3	14.985	1177500	1260745	1952.9022

4. PERFORMANCE PARAMETERS WITH BEARINGS

The load components in the x too y directions can be situated calculated by way of follows [17]:

$$F_y = \iint_{A_j} P_j \cdot \cos\theta \cdot (dA_j) \tag{14}$$

$$F_x = \iint_{A_i} P_i \cdot \sin\theta \,.\, (dA_i) \tag{15}$$

a - mesh details of the fluid domain

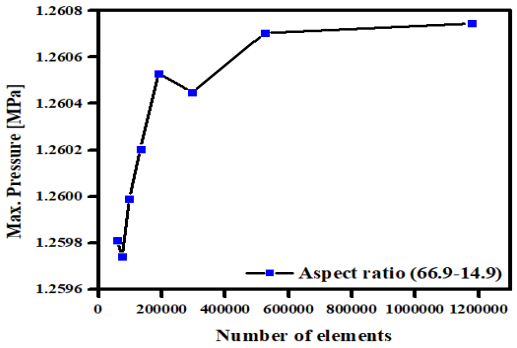

b – pressure parameter

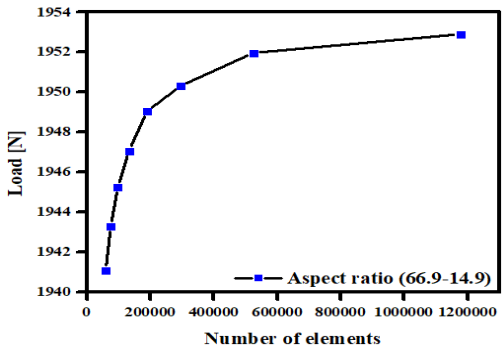

c – load parameter

Fig. 2. Convergence test

The bearing's total load can be calculated as follows [17]:

$$W = \sqrt{(F_x)^2 + \left(F_y\right)^2} \tag{16}$$

The following formula can be used to determine the attitude angle [17]:

$$\phi = \tan^{-1}\left(\frac{F_y}{F_x}\right) \tag{17}$$

The following formula can be used to determine the friction force at the journal surface [18]:

$$F_{fr} = \iint \tau \cdot (dA) \tag{18}$$

5. BOUNDARY CONDITIONS

5.1. Flow field boundary conditions

The inlet and outlet pressures of the bearing was assumed to be atmospheric pressure, stationary bearing housing, rotating journal interface with

different speeds (1000-3000) rpm, elastic wall housing.

5.2. Thermal boundary conditions

Inlet and outlet temperature was assumed to be 313K at the coupled bearing interface.

6. SOLUTION METHODOLOGY

In the first part, the meshed model is fed into the Fluent, and the journal bearing parameters and lubricant properties are set. The fluid domain's operational parameters, including the original pressure and temperature ground, are then specified. To determine the pressure and temperature distributions as well as the flow velocities, the continuity, momentum, and energy equations must be solved. Additionally, the fluid-structure crossing point environment organization, which executes the would-be-coupling design amid the liquid and solid domains, realizes the data exchange of fluid-construction edges. In the meantime, it is possible to establish the solid domain's operational conditions and to resolve its governing equations. The procedure was then repeated until convergence was attained, as depicted in figure 3. Under steady state, laminar flow conditions, the effects of flow regime on the lubrication performance of the journal bearings were investigated. The governing equations are resolved with three-dimensional accuracy. The CFD analysis employs the SIMPLE-C algorithm for pressure-velocity coupling. A two-phase mixture model using the multiphase theory is applied, and its vaporization pressure is set at 29185 Pa.

7. DISCUSSION OF THE RESULTS

This section will present and discuss the static properties of flexible journal bearings that have been lubricated with various lubricants. At various values of eccentricity ratio (0.1 to 0.8) and various values of journal speed, performance characteristics including maximum pressure, load-carrying capacity, friction force, and maximum temperature have been evaluated (1000-3000).

7.1. Validation of the CFD model

The distribution of oil film temperature determined by the current study was compared to that determined by Ferron et al. (1983) [16], as depicted in figure (4). This graph demonstrates the strong correlation between the two distributions of oil film temperature, with a maximum variance of 1.26 percent.

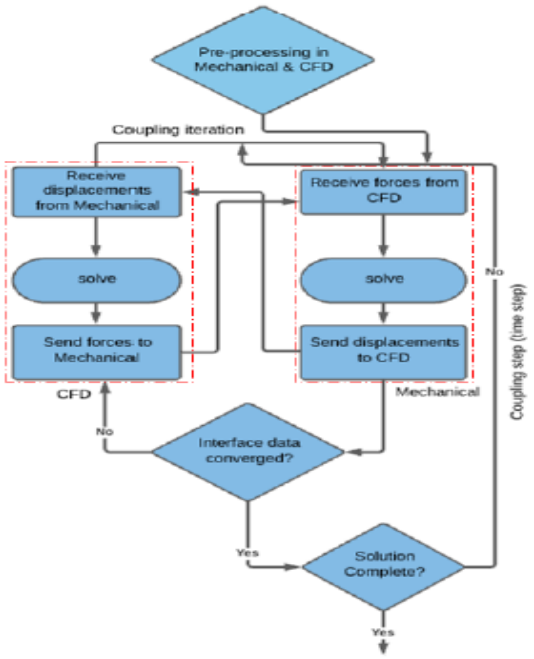

Fig. 3. Flow Chart of two way FSI

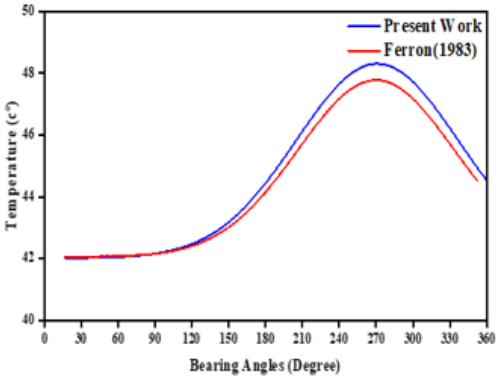

Fig. 4. Distribution of bearing temperature

7.2. Thermal effect on the bearing performance

Thermal oil film pressure of the bearing was compared with that obtained from the isothermal model when it was lubricated with SAE10W50 and SAE15W40 lubricants and works at a 0.5 eccentricity ratio, as demonstrated in Figure (5). This graph makes it evident that when the oil film temperature rises, the oil viscosity of the oil decreases, which results in a drop in the oil film pressure.

A lower drop in the pressure of lubricant film was found after the lubricated bearing by SAE15W40 rather than SAE10W50. Figure 6 shows how the temperature of the oil film rises with the variety of oil lubricants. Because SAE10W50 oil has a higher viscosity than SAE15W40 oil, which consequences in a advanced lubricant shear stress, the oil film temperature increases once the bearing is oiled with SAE10W50 oil rather than SAE15W40 oil, as shown in the graph.

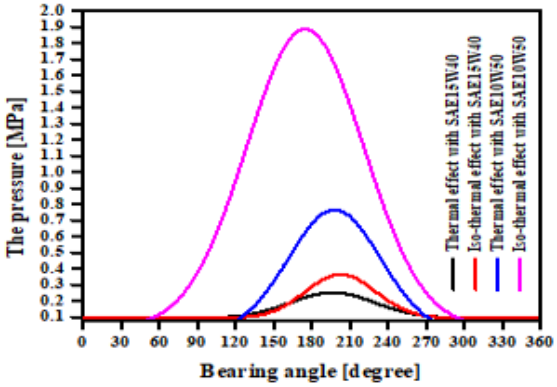

Fig. 5. Thermal and isothermal circumferential bearing pressure distribution

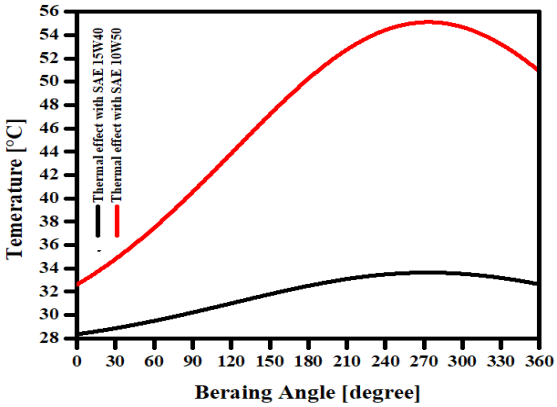

Fig. 6. Temperature oil film distribution

The combined effect of journal speed and the oil viscosity on the load carrying capacity of the bearing is presented in figure (7). This graph shows how, as journal speeds increase, the load supported through the bearing increases. This figure also showed that the decrease in oil viscosity caused by the rise in oil film temperature had a minor impact on the load carried by the bearing that was lubricated with SAE15W40. When a bearing is lubricated with SAE10W50 and rotates at a journal speed of 3000 rpm, it has been observed that the load it supports falls by about 15%.

Figure illustrates how the effect of the oil film temperature on the friction force at the bearing surfaces decreases (8). This is explicable by the lower oil viscosity under this circumstance which leads to lower shear rate and shear stress. It can be expressed that the bearing greased by SAE10W50 lubricant induced graeter friction force than that lubricated with SAE15W40 due to the higher viscosity of the former than the later.

It is also obvious that the higher shear rate and resulting shear stress in this situation cause the friction force generated at the bearing surfaces to increase as the journal speed of the bearing increases.

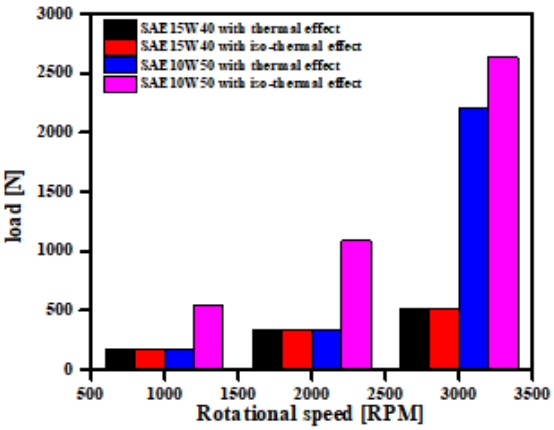

Fig. 7. The Load Carried of the Bearing vs. Different Journal Speeds

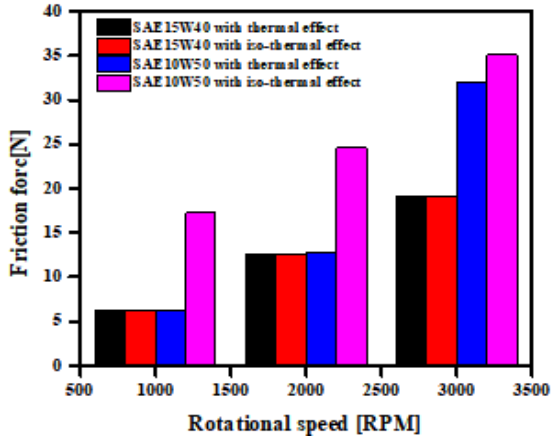

Fig. 8. The Friction force vs. Journal Speeds

7.3. Cavitation effect

As shown in Figure 9, which depicts the thermal pressure distribution for a bearing operating at journal speed of 3000rpm and eccentricity ratio of 0.5 and lubricated with 10W50 oil, the extreme pressure of the lubricant film decreases as the cavitation outcome interacts with the other effects. This occurred as a result of the density and the two-phase (liquid-gas) viscosity lubricant decreasing, which had an impact on the viscous period of the Navier Stocks equivalences. The maximum reduction in oil film pressure that results from taking the cavitation effect into account when the bearing operates at various rotational speeds is shown in Figure 10. In Figure 11, the bearing greased with SAE10W50 obviously carries a heavier load than the bearing lubricated with SAE15W40. A bearing's increase in load carrying capability is greater when it runs at higher eccentricity ratios. This figure also demonstrates that the load supplied by the bearing reduces when the cavitation effect is considered after the behavior of the pressure lubrication film. Figure shows how the journal outward urged friction force behaved when the combined effects of the oil viscosity and cavitation were taken into consideration (12). Due to the higher viscosity of SAE10W50 compared to SAE15W40, it can be located seen that the induced resistance force in the

bearing is greater when it is lubricated with the former. The induced friction force has lower values when the cavitation effect was considered due to the lower viscosity of the two- phase lubricant produced in the cavitated zone. Figure13 clearly demonstrates that when the cavitation effect was taken into account, the maximum oil film temperature decreased. This is explained by the fact that the lubricant contains air bubbles, which causes the lubricant to behave as a two-phase flow and results in lower oil viscosity and density.

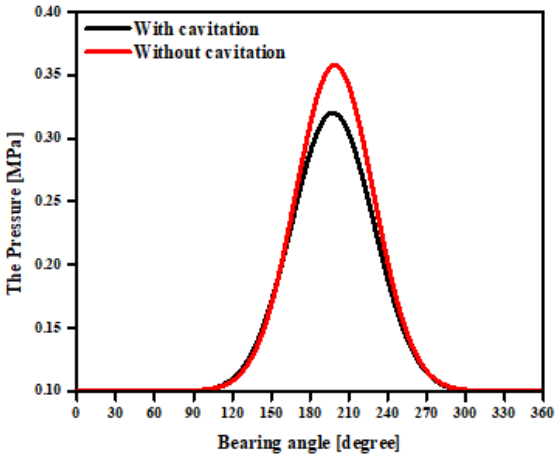

Fig. 9. Cavitation effect on circumferential pressure distribution

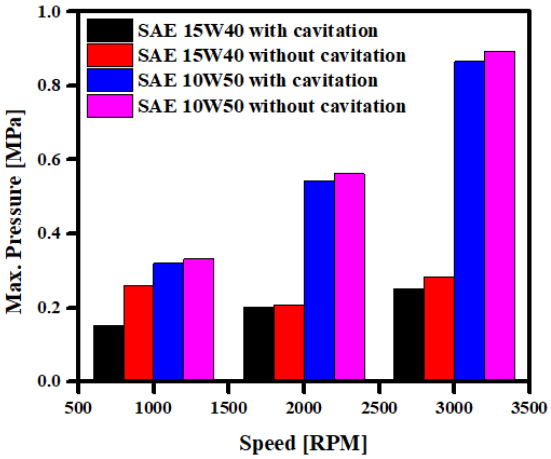

Fig. 10. The effect of journal speed and cavitation on maximum pressure

7.3. The effect of elastic deformation

The effect of the elastic deformation of the bearing material on the different bearing characteristics was investigated with the fluid-structure interaction method. It was put into practice by first using (CFD) connecting the structure to the forces and vice versa. Figure 14 shows the combined effects of thermal and elastic deformation on the oil film pressure of a journal bearing that was lubricated with SAE 15W40 and SAE 10W50 lubricants and operating at a rotational speed of 3000 rpm and an eccentricity ratio of 0.5. Figure 15 compares the maximum thermal oil film pressure for a bearing with rigid and elastic bearing materials while it works at 0.5 eccentricity ratio and varied journal speeds. This graph makes it abundantly evident that when the elastic deformation of the bearing liner is taken into account, the lubrication pressure decreases in contrast to that obtained for a rigid bearing. This is due to a decrease in film pressure brought on by a thickening of the oil film. The active area of the bearing increases and the cavitation area decreases, showing a larger load-carrying capability in this instance when the elastic deformation of the bearing liner is disregarded.

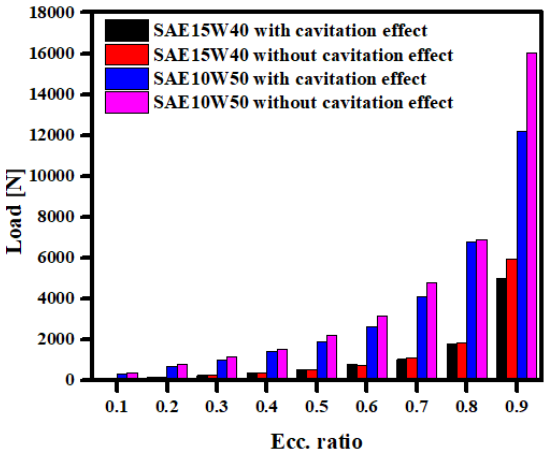

Fig. 11. Effects of cavitation on the bearing load at different Ecc..ratios

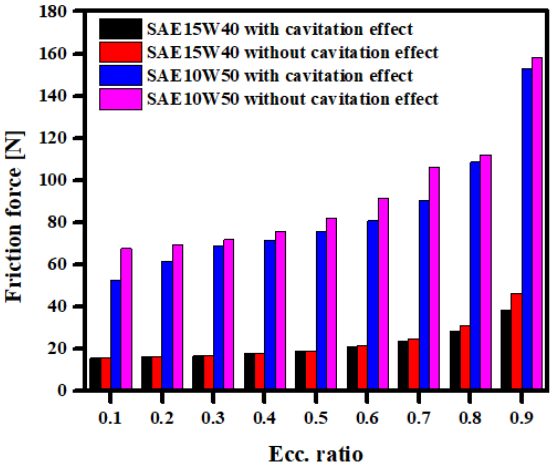

Fig. 12. Effect of Friction force vs. Different Ecc. ratio

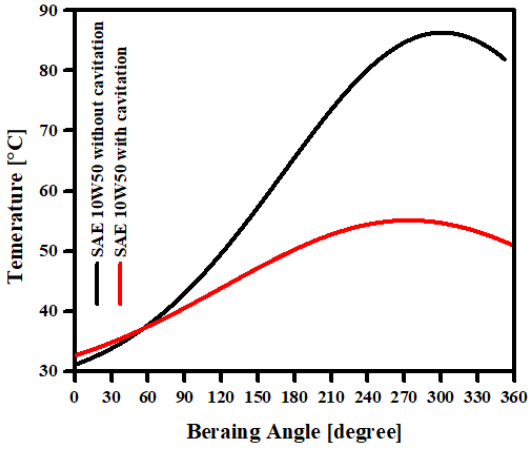

Fig. 13. Effect of cavitation on the oil film temperature distribution

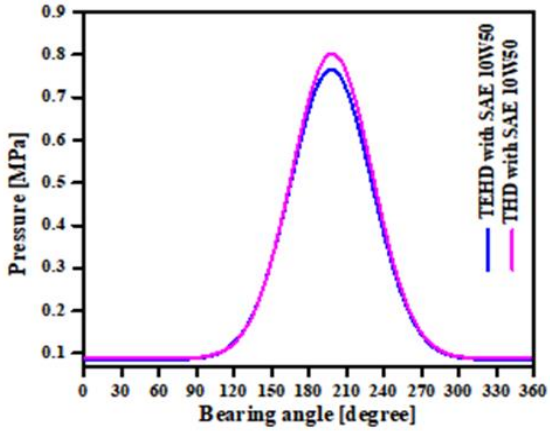

Fig. 14 Thermal effect on bearing pressure distribution

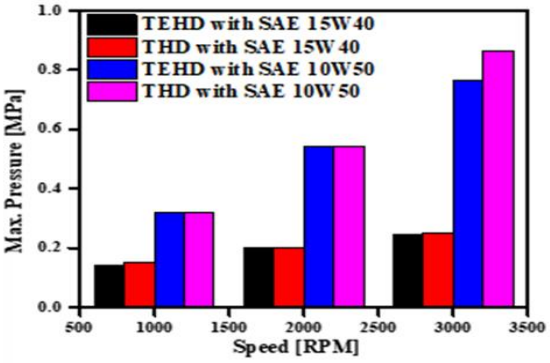

Fig. 15. Effects of oil film temperature on the maximum pressure

This leads to the main conclusion that the bearing material's elastic deformation has a significant impact on the generated oil film pressure and, as a result, the main bearing parameters, and should not be overlooked by the designers in order to achieve reasonable results. Figure illustrates the total flexible deformation material of the bearing after it had been greased with various types of lubricants and operated at various eccentricity ratios (16). This graph demonstrates that once it operates at larger eccentricity ratios, the bearing lubricated with SAE10W50 experiences significant elastic deformation of the bearing material. This can be attributed to the situation's increased oil film pressure, which increases the lubricant film forces acting on the bearing surface. When a bearing operates at eccentricity ratios below 0.6, the type of oil used to lubricate the bearing has a small impact on the elastic deformation of the bearing material. This is seen in Figure (17), which shows how the speed journal affects the elastic deformation of the bearing material when it is lubricated with various lubricants and operating at 0.5.

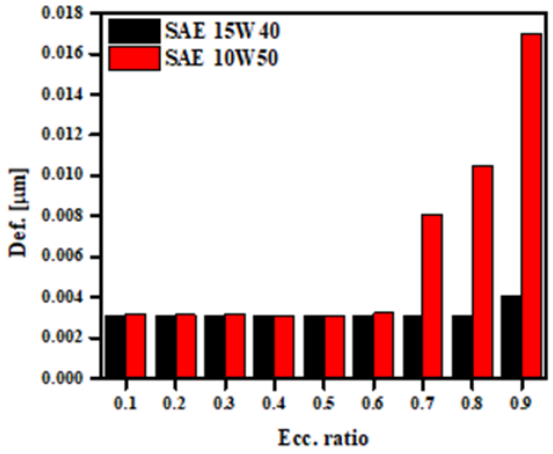

Fig. 16. Bearing material deformation vs. eccentricity ratio

Figures 18 and 19 show the load carried by the bearing determined by utilizing TEHD and THD solutions for a bearing that operates at various eccentricity ratios and speeds. In general, the load borne by the bearing increases with increased eccentricity ratio and speed, but it reduces when elastic deformation of the bearing shell is taken into account. The primary cause of this behavior is the reduced oil film pressure brought on by the greater oil film thickness obtained in this instance. Figures 20 and 21 show that the resistance force produced at the bearing exteriors marginally lowers when bearing elastic deformation is taken into account. The bearing ran at varied speeds while being lubricated with SAE15W40 and SAE10W50 lubricants at various eccentricity ratios and speeds. This can be explained by the oil film thickening, which causes a decrease in the friction force, shear rate, and shear stress. The volume proportion of the gas phase at the cavitation zone increases as the journal speed of the bearing increases, as seen in figure 22. (a,b,c). This figure displays the volume fraction distribution while the bearing rotates at 1000, 2000, and 3000 rpm. As the rotational speed rises, the cavitation area gradually expands. The pressure of the created oil film is still higher, though.

8. CONCLUSIONS

Computational Fluid Dynamics was used to perform thermo-elasto-hydrodynamic analysis of circular journal bearings when it was lubricated with different types of oil.

1. When the viscosity is maintained constant, the temperature rise in the lubricant is greater, as is the maximum pressure obtained. When the temperature rises, the viscosity of the lubricant decreases, reducing the bearing's load-carrying capacity.
2. The lubricant pressure reductions after the effect of cavitation is considered.
3. The current analysis could help predict bearing performance parameters in real-world conditions and extend bearing life.

4. The bearing characteristics decrease when the elastic deformation of the bearing liner is taken into account.
5. The bearing material deforms more when it is used at higher eccentricity ratios and rotating speeds .

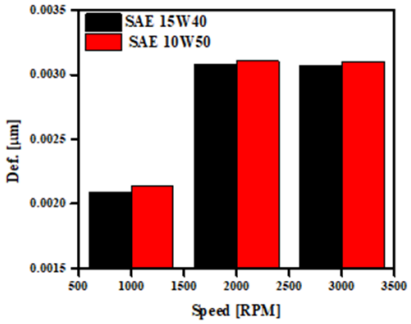

Fig. 17. The deformation of the Bearing vs. rotational speed.

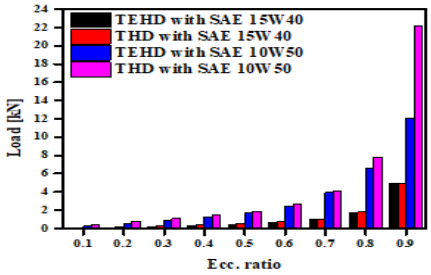

Fig.18. The load carrying capacity vs. eccentricity ratio.

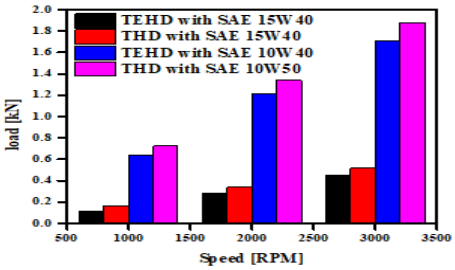

Fig. 19. The load carrying capacity vs. rotational speed.

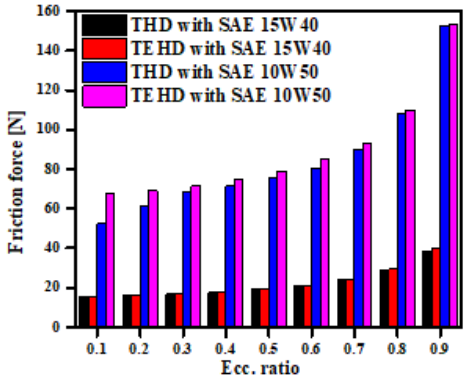

Fig. 20. The friction force vs. eccentricity ratio

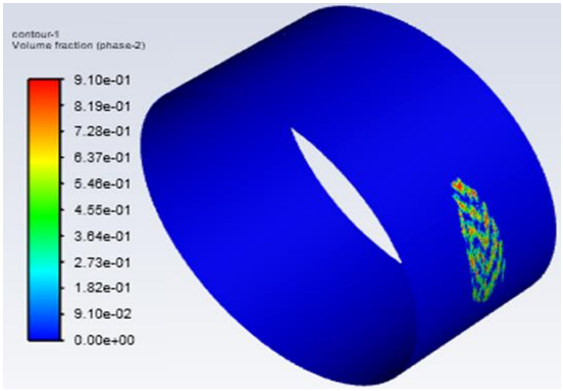

(a) – at rotational speed = 1000 rpm

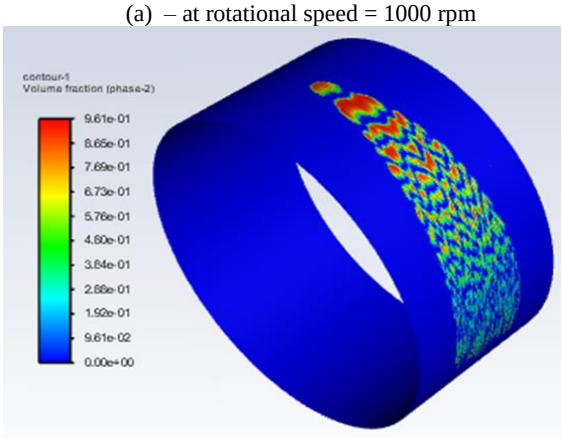

(b) at rotational speed = 2000 rpm

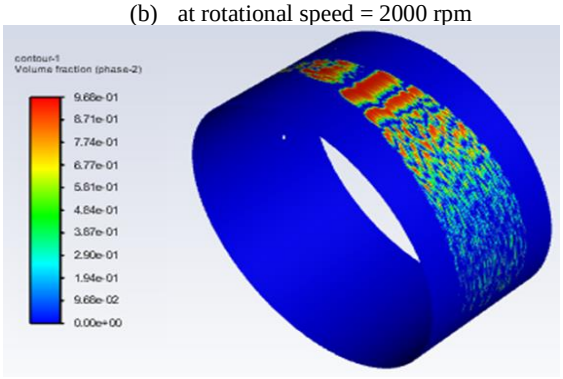

(c) - at rotational speed = 3000 rpm

Fig. 22. Rotational speed effect on the volume fraction of the gas phase.

Author contributions: *research concept and design, Z.K.; Collection and/or assembly of data, Z.K.; Data analysis and interpretation, Z.K.; Writing the article, L.A-A.; Critical revision of the article, F.R.; Final approval of the article, A.R.*

Declaration of competing interest: *The authors declare that they have no known competing financial interests or personal relationships that could have appeared to influence the work reported in this paper.*

REFERENCES

1. Nour AM. An experimental investigation of hydrodynamic journal bearing with different oil grades. Port-Said Engineering Research Journal 2019; 23(2):46-54. http://dx.doi.org/10.21608/pserj.2019.49576.
2. Srinivas, Yunnus M, Munshi SM, Hussain IH. Performance evaluation of hydrodynamic journal

bearing using gearbox and engine oil (SAE90 and SAE20w50) by experimental and theoretical methods. International Journal of Mechanical Engineering and Information Technology 2015; 3(11): 1573-1583. http://dx.doi.org/10.18535/ijmeit/v3i11.04.
3. Baskar S, Sriram G. Tribological behavior of journal bearing material under different lubricants. Tribology in Industry 2014; 36(2): 127-133.
4. Lorenz N, Offner G, Knaus O. Thermal analysis of hydrodynamic lubricated journal bearings in internal combustion engines. Proceedings of the Institution of Mechanical Engineers, Part K: Journal of Multi-body Dynamics 2017;231(3):406-419. https://doi.org/10.1177/1464419317693878.
5. Chauhan A, Sehgal R, Sharma RK. Thermohydrodynamic analysis of elliptical journal bearing with different grade oils. Tribology International 2010;43:1970–1977. https://doi.org/10.1016/j.triboint.2010.03.017.
6. Williamson BP, Walters K, Bates TW, Coy RC, Milton AL. The viscoelastic properties of multigrade oils and their effect on journal-bearing characteristics. Journal of Non-Newtonian Fluid Mechanics 1997; 73(1-2): 115-126. https://doi.org/10.1016/S0377-0257(97)00039-6.
7. Rasep Z, Yazid MNAWM, Samion S. A study of cavitation effect in a journal bearing using CFD: A case study of engine oil, palm oil and water. Jurnal Tribologi 2021; 28: 48-62.
8. Muchammad, Tauviqirrahman M, Soetopo HSS, Jamari. Mechanical and thermal deformations effects on plain journal bearing with isoviscous boundary condition based on CFD and FSI methods. Jurnal Tribologi 2021; 28: 63-81.
9. Liu H, Xu H, Ellison PJ, Jin Z. Application of computational fluid dynamics and fluid–structure interaction method to the lubrication study of a rotor–bearing system. Tribology Letters 2010; 38(3): 325-336. https://doi.org/10.1007/s11249-010-9612-6.
10. Singla A, Kumar A, Bala S, Singh P, Chauhan A. Thermo-hydrodynamic analysis on temperature profile of circular journal bearing using computational fluid dynamics. 2014 Recent Advances in Engineering and Computational Sciences (RAECS). IEEE 2014; 1-6. https://doi.org/10.1109/RAECS.2014.6799595.
11. Chen Y, Sun Y, He Q, Feng J. Elastohydrodynamic behavior analysis of journal bearing using fluid–structure interaction considering cavitation. Arabian Journal for Science and Engineering 2019; 44(2): 1305-1320. https://doi.org/10.1007/s13369-018-3467-9.
12. Chauhan A. Circular bearing performance parameters with isothermal and thermo-hydrodynamic approach using computational fluid dynamics. International Journal of Research in Advent Technology 2014; 2(7): 46-52.
13. Versteeg HK, Malalasekera W. An introduction to computational fluid dynamics: the finite volume method. Pearson education 2007.
14. Zwart PJ, Gerber AG, Belamri T. A two-phase flow model for predicting cavitation dynamics. Fifth international conference on multiphase flow 2004; 152.
15. Gertzos KP, Nikolakopoulos PG, Papadopoulos CA. CFD analysis of journal bearing hydrodynamic lubrication by Bingham lubricant. Tribology international 2008;41(12):1190-1204. https://doi.org/10.1016/j.triboint.2008.03.002.
16. Ferron J, Frene J, Boncompain R. A study of the thermohydrodynamic performance of a plain journal bearing comparison between theory and experiments. Journal of Lubrication Technology 1983; 105(3): 422-428. https://doi.org/10.1115/1.325463.
17. Dhande DY, Pande DW. A two-way FSI analysis of multiphase flow in hydrodynamic journal bearing with cavitation. Journal of the Brazilian Society of Mechanical Sciences and Engineering 2017; 39(9): 3399-3412. https://doi.org/10.1007/s40430-017-0750-8.
18. Abass BA, Ahmed SY, Kadhim ZH. Thermoelasto-hydrodynamic analysis of nano-lubricated journal bearings using computational fluid dynamics with two-way fluid–structure interaction considering cavitation. Arabian Journal for Science and Engineering 2022;48:2939-2950. https://doi.org/10.1007/s13369-022-07024-9.

Received 2023-01-03
Accepted 2023-05-12
Available online 2023-05-28

Zainab H. Kadhim was born in 1996 in the Iraqi city of Kut. She holds a bachelor's degree in mechanical engineering from the University of Babylon in 2018 and a master's degree. From the University of Babylon, College of Engineering, Department of Mechanical Engineering in 2022.

Lekaa Hammed was born in Baghdad, Iraq in 1974. She received the B.Sc. degree in Mechanical engineering from the University of Babylon, in 1996. She is working in university of Babylon, college of engineering, mechanical engineering department from 1999 till now. She received the M.Sc. in Mechanical Engineering in 2006 from the University of Babylon. Her Scientific title lecturer from 2009 till now at the university of Babylon, College of Engineering, Department of Mechanical Engineering. She has Exact scientific expertise in applied mechanics, tribology, Machine design.

Fatima Rahima was born in 1996 in the Iraqi city of Amarah. She holds a bachelor's degree in mechanical engineering from the University of Babylon in 2018 and a master's degree. From the University of Babylon, College of Engineering, Department of Mechanical Engineering in 2022.

Ali Mohammed Ridha
Work Experience:
Ministry of Health – Iraq- Governmental Sector 2019-Present
Ministry of Higher Education and Scientific Research 2017-2019
Education & Qualifications
2018-2020 Middle Technical University
MSc Medical Electronic Instrumentation Techniques Engineering
2012-2016 AL Hussain University College
BSc Medical Instrumentation Techniques Engineering